

New computational algorithms for the Limit Analysis of large-scale 3D truss-frame structures

***Rosalba Ferrari¹, Giuseppe Cocchetti^{1,2}, and **Egidio Rizzi¹**

¹ Università degli Studi di Bergamo, Dipartimento di Ingegneria e Scienze Applicate
viale G. Marconi 5, I-24044 Dalmine (BG), Italy

² Politecnico di Milano, Dipartimento di Ingegneria Civile e Ambientale
piazza L. da Vinci 32, I-20133 Milano, Italy

*Presenting author: rosalba.ferrari@unibg.it

**Corresponding author: egidio.rizzi@unibg.it

Abstract

Two new computational algorithms for the Limit Analysis (LA) of large-scale 3D truss-frame structures recently proposed by the authors are reconsidered and adapted for a comparison prediction of the elastoplastic response of a strategic beautiful historic infrastructure, namely the Paderno d'Adda bridge, a riveted wrought iron railway viaduct that was built in northern Italy in 1889. The first LA algorithm traces a fully exact evolutive piece-wise linear elastoplastic response of the structure, up to collapse, by reconstructing the true sequence of activation of made-available plastic joints (as a generalization of plastic hinges), in the true spirit of LA. The second LA algorithm develops an independent kinematic iterative approach apt to directly determine the plastic collapse state, in terms of collapse load multiplier and plastic mechanism, based on the upper-bound theorem of LA. Specifically, the marvelous doubly-built-in parabolic arch of the bridge is analyzed, under a static loading configuration at try-out stage, and its elastoplastic response is investigated, in terms of evolutive load-displacement curve, collapse load multiplier and plastic collapse mechanism. The two LA algorithms are found to much effectively run and perform, despite for the rather large size of the computational model, with a number of dofs in the order of four thousand, by achieving good corresponding matches in terms of the estimate of the load-bearing capacity and of the collapse characteristics of the arch substructure, showing this to constitute a well-set structural element. Moreover, the direct kinematic method displays a rather dramatic performance, in truly precipitating from above on the collapse load multiplier and rapidly adjusting to the collapse mode, in very few iterations, by a considerable saving of computational time, with respect to the complete evolutive elastoplastic analysis. This shall open up the way for a further adoption of such advanced LA tools, with LA regaining a new momentum within the optimization analysis of structural design and form-finding problems.

Keywords: Limit Analysis (LA), evolutive elastoplastic response, kinematic (upper-bound) theorem, collapse load multiplier, plastic collapse mechanism, truss-frame structures, historic construction

1. Introduction

Limit Analysis (LA) constitutes by today a well-established and consolidated discipline, for evaluating consistent bounds on the collapse (limit) loads acting on engineering structures characterized by a mechanical behavior that may be idealized as perfectly plastic, subjected to constant permanent loads and increasing live loads.

LA may be considered as a milestone in the more recent history of structural mechanics and provides a rather powerful tool for structural design and assessment purposes, within a wide variety of engineering situations. It has acquired its rational formulation thanks to the contribution by Drucker et al. [1], who have formulated and demonstrated the fundamental theorems of LA for a continuum. More recent consolidated contributions, such as those by Massonet and Save [2], Kaliszky [3], Lubliner [4], Jirasek and Bazant [5], and many others, as those quoted in Maier et al. [6], have further made the theory and the methods of LA rather fundamental in various applications of mechanics of solids and structures, becoming by now classical references on the topic. LA of frames has also been revived in recent years, with several interesting applications (see e.g. Cocchetti and Maier [7], Tangaramvong and Tin-Loi [8], Lògò et al. [9], Skordeli and Bisbos [10], Bleyer and Buhan [11], Nikolaou et al. [12]), despite, basically being employed at an academic level, somehow still far from implementations within the engineering profession.

A new impetus toward the application of the LA discipline within structural engineering has been recently targeted by the authors by two different proposals, respectively in Ferrari et al. [13,14] and in Ferrari et al. [15], with reference to the structural elastoplastic analysis of large-scale 3D truss-frame structures. The effort was motivated by the goal of performing an effective LA of the collapse state of a strategic and historic truss-frame infrastructure, as described below. In former contribution Ferrari et al. [13,14], a computational algorithm for tracing the “exact” piece-wise linear evolutive elastoplastic response of the structure up to collapse in the true spirit of LA has been formulated and implemented. In latter attempt Ferrari et al. [15], a kinematic upper-bound LA direct method of computational analysis has been proposed, allowing to iteratively converge on the collapse state in terms of collapse load multiplier and plastic mechanism.

In the work herein presented, such two new approaches are employed toward the LA analysis of a large truss-frame substructure displaying a rather considerable complexity, namely a 3D model of the box-formed doubly-built-in parabolic arch of the Paderno d’Adda bridge (1889), a beautiful monumental infrastructure in the local territory. This roughly involves 1,050 beam finite elements with potentially active plastic joints and more than 4,000 degrees of freedom.

In the paper, it is shown that the kinematic algorithm rapidly converges onto the collapse state, as also traced by the full evolutive elastoplastic analysis, with a kinematic load multiplier that quickly precipitates from above on the sought collapse load amplifier and a plastic mechanism that rapidly adjusts to the true collapse one. The kinematic algorithm has proven to display a saving of more than 96% of the computational time employed for the evolutive elastoplastic analysis, which additionally reconstructs the whole sequence of activation of the plastic joints and traces a rather ductile piece-wise linear load-displacement curve, showing the arch to constitute a beautiful well-designed structural element, in terms of load-carrying capacity up to the limit state of plastic collapse.

The present paper is structured as follows. Section 2 briefly introduces the two developed LA algorithms. Section 3 illustrates the results achieved from the numerical analyses conducted on the truss-frame parabolic arch of the Paderno d’Adda bridge. Brief comments on the various computational aspects and the effectiveness of the performed simulations are concisely pointed out in the Conclusions.

2. Limit Analysis formulation

The two computational formulations herein adopted are based on the same underlying hypotheses, as briefly listed here. Perfectly-plastic joints have been located at the two edges of each beam finite element composing the model structure; a piece-wise linear yield domain,

specifically an uncoupled Rankine-type boxed-form yield domain in the space of the static variables (i.e. beam internal actions), is chosen. Linear kinematics is assumed, namely second-order non-linear geometrical effects are ruled out and equilibrium is enforced in the initial (unstressed) configuration of the structure. Permanent (i.e. gravity) loads and a set of (basic) loads amplified by a common (“load multiplier”) factor are considered.

Both formulations have been implemented within MATLAB[®], with specific computer programs exploiting 3D beam finite elements. Exact time integration is one of the main characteristics of the evolutive elastoplastic formulation (see e.g. Ferrari et al. [13,14]). The kinematic algorithm of Limit Analysis, discussed in Ferrari et al. [15], and prodromal references quoted therein, is based on a kinematic upper-bound approach and is below newly applied to a large-scale 3D truss-frame structure, for comparison purposes with the former evolutive elastoplastic algorithm.

2.1. Evolutive elastoplastic approach

The evolutive LA elastoplastic approach proposed in Ferrari et al. [13,14] relies on an iterative procedure in which the global elastoplastic matrix of the structure is iteratively updated, based on the plastic modes that become active during the increment of the applied live loads. In this way, the characteristic non-linear (piece-wise linear) load/displacement response curve is estimated, up to collapse.

A synthesis of the main characteristics of the computational algorithm can be outlined as follows. In the approach, the kinematic constraints on the structural system are imposed by enforcing the stationary condition of Lagrangian function \mathcal{H} :

$$\mathcal{H}(\mathbf{U}, \mathbf{R}) = \frac{1}{2} \mathbf{U}^T \mathbf{K} \mathbf{U} - \mathbf{F}^T \mathbf{U} - \mathbf{R}^T (\mathbf{C} \mathbf{U} - \mathbf{V}) \quad (1)$$

where vector \mathbf{U} collects all the nodal dofs of the system, matrix \mathbf{K} is obtained by a classical assembly procedure of the finite element stiffness matrices, and vector \mathbf{F} is created as the assembly of the equivalent nodal force vectors, including only the active loads. In Eq. (1), constraint equations $\mathbf{C} \mathbf{U} = \mathbf{V}$ are imposed: matrix \mathbf{C} depends only on geometrical quantities, vector \mathbf{V} collects possible given values of the kinematic quantities, vector \mathbf{R} gathers the so-called *Lagrangian multipliers*, which may be interpreted, from a mechanical point of view, as the reactions supplied by the constraints.

The solution of the structural system is derived from Eq. (1), and by applying a Gaussian elimination to the system of the constraint equations, in order to eliminate those, among the latter, that are just a repetition of others. If this occurs, the elimination procedure leads to a reduced system, from which the solution in terms of (independent) displacements (\mathbf{u}) can be symbolically given by the following expression:

$$\mathbf{u} = \mathbf{K}_{uu}^{-1} (\mathbf{F}_D + \mathbf{F}_u) \quad (2)$$

where \mathbf{K}_{uu} is a reduced stiffness matrix and \mathbf{F}_D and \mathbf{F}_u are reduced known-term vectors, derived through appropriate mathematical steps, from vector \mathbf{V} and vector \mathbf{F} , respectively (see Ferrari et al. [13] for the details).

The evolutive approach is based on an incremental procedure that can be outlined as follows:

- (i) At the beginning of the analysis, the structure is not under the effect of loading or of pre-existing stress states; then, there is no plasticization in the structure (no yield plane is active). Afterwards, the following quantity is set acting on the structure: $\Delta \mathbf{F}_{Li} = \Delta \alpha \mathbf{F}$, where $\Delta \mathbf{F}_{Li}$ represents the load increment, determined from \mathbf{F} through load factor $\Delta \alpha$,

which is always positive and can be assumed as a chronological variable in the increment of \mathbf{F} ;

- (ii) Given $\Delta\mathbf{F}_{Li}$, also quantity $\Delta\mathbf{F}_u$ can be determined. Then, substituting the latter into Eq. (2), the incremental solution in terms of displacements $\Delta\mathbf{u}$ is thus provided. It is worth to note that at the beginning of the procedure matrix \mathbf{K}_{uu} is totally elastic;
- (iii) Being $\Delta\mathbf{u}$ strictly related to the increment of the static internal variables of each finite element ($\Delta\mathbf{N}$), the latter can also be computed. Incremental solutions $\Delta\mathbf{u}$ and $\Delta\mathbf{N}$ do not take into account that some modes may be possibly activated during the step; on the other hand, it is possible that the extent of incremental load $\Delta\mathbf{F}_{Li}$ is not enough to determine the reaching of at least one internal static variable in a section on the corresponding yield limit. Through a comparison between each static internal variable at the beginning of the step and the corresponding yield limit, the procedure calculates for each mode, among all non-activated ones, the specific *scale factor* (β) of incremental load $\Delta\mathbf{F}_{Li}$ leading to possible activations. The minimum among all such estimated factors, $\gamma = \min\{\beta\}$, allows to get the *exact* extent of the current step to achieve new activation(s);
- (iv) Through coefficient γ , the original incremental solution is proportionally rescaled, and the static and kinematic quantities of the structure at the end of the step are updated;
- (v) At the end of the step some yield planes (at least one) are now activated and stiffness matrix \mathbf{K}_{uu} becomes elastoplastic. Its determination is computed through a convenient Gaussian elimination procedure, which represents a peculiar feature of the implemented evolutive approach (see Ferrari et al. [13] for a comprehensive description of the computational formulation).

The whole procedure assumes an iterative configuration in the repetition of steps (ii)-(v). It stops when the collapse of the structure is reached, namely when the minimum eigenvalue of global (updated) matrix \mathbf{K}_{uu} calculated within step (ii) vanishes (or it is below a given numerical tolerance) and the eigenvector is everywhere associated to a positive load dissipation (Ferrari et al. [13]).

2.2. Kinematic upper-bound direct method

A synopsis of the principal features of the computational algorithm outlined in Ferrari et al. [15] is recalled below.

The direct LA kinematic method is distinguished from other kinematic approaches due to its alternative and elegant formulation, which provides a very convenient procedure for the LA of truss-frames. According to the upper-bound (kinematic) theorem, the *kinematic load multiplier* is defined as follows:

$$\mu_k = \frac{\dot{L}_i - \dot{L}_e^g}{\dot{L}_e^0} \quad (3)$$

where \dot{L}_i represents the internal power dissipation of the structure, \dot{L}_e^g and \dot{L}_e^0 represent the power of the base live loads and the power produced by the permanent loads applied to the structure, respectively. A corollary of the upper-bound theorem states that the collapse load multiplier is the minimum among the kinematic load multipliers defined for whole set K of the kinematically admissible mechanisms, namely $\mu_c = \min_K \{\mu_k\}$. Being \dot{L}_i and \dot{L}_e homogeneous functions of order one with respect to the velocity field, $\dot{L}_e^0 = 1$ can always be

set for a kinematically admissible mechanism (M); thus, the collapse load multiplier can be obtained as the solution to the following constrained optimization problem:

$$\mu_c = \min_{M \in C} \left\{ \dot{L}_i(M) - \dot{L}_e^g(M) \mid \dot{L}_e^0(M) = 1 \right\} \quad (4)$$

If the minimization is limited to a subset of compatible mechanisms $\bar{C} \subseteq C$, it results:

$$\mu_c \leq \mu_k = \min_{M \in \bar{C}} \left\{ \dot{L}_i(M) - \dot{L}_e^g(M) \mid \dot{L}_e^0(M) = 1 \right\} \quad (5)$$

For instance, with reference to the structure discretization, this can happen when the collapse mechanism requires an active plastic joint within one or more beam elements, besides the plastic joints at the beam ends.

The procedure proposed by Ferrari et al. [15] exploits a convenient reshaping of the internal power dissipation description of a beam element, in order to adapt an existing efficient approach originally presented by Zhang et al. [16], for the LA of continua, within the classical FEM analysis based on beam element discretization. In particular, the procedure adopts a *quadratic form* of the internal power dissipation of a beam element, whose expression turns out to be defined as follows:

$$\dot{L}_i(\dot{\mathbf{q}}) = \dot{\mathbf{q}}^T \mathbf{S}(\dot{\mathbf{q}}) \dot{\mathbf{q}} \quad (6)$$

where vector $\dot{\mathbf{q}}$ lists the nodal velocities of the structure and matrix $\mathbf{S}(\dot{\mathbf{q}})$ is a function of: (a) the generalized plastic strains of all the beams that form the structure (the axial and the transverse relative rotations and the axial relative displacement, for each joint); (b) the corresponding internal actions activating the plastic strains (torque, two bending moments and axial force, for each joint). Matrix $\mathbf{S}(\dot{\mathbf{q}})$ thus governs the global internal power dissipation of the structure; it is symmetric, highly sparse (even narrow-banded with a proper numbering of dofs) and positive definite (or positive semidefinite when non-dissipative rigid-body motions are allowed by constraints), namely the same properties characterizing the classical global stiffness matrix for an elastic FEM frame analysis.

The direct LA kinematic method is based on an iterative procedure that can be outlined as follows:

- (i) At the beginning of the analysis, vector $\dot{\mathbf{q}}_0$ is set up by a vector of random numbers and normalized in order to guarantee that $\dot{L}_e^0(\dot{\mathbf{q}}_0) = 1$;
- (ii) Let one now consider iteration $n+1$. Vector of nodal velocities $\dot{\mathbf{q}}_n$ relevant to the n -th iteration (still normalized in order to guarantee that $\dot{L}_e^0(\dot{\mathbf{q}}_n) = 1$) and corresponding load amplification factor μ_k^n are assumed to be known, the last one computed through Eq. (3). Then, the iterative process leads to generate a new mechanism, governed by new vector $\dot{\mathbf{q}}_{n+1}$ that is obtained as the solution of the quadratic constrained minimization problem in Eqs. (5)-(6), in which the internal power dissipation, given by Eq. (6), is computed through coefficient matrix $\mathbf{S}_n = \mathbf{S}(\dot{\mathbf{q}}_n)$, related to previous iteration n . The resulting constrained minimization problem can be solved by enforcing the stationarity condition on a Lagrange function, in this way leading to a set of two equations, each one to be a function of an unassigned variable, namely $\dot{\mathbf{q}}$ and λ , respectively, being the latter a *Lagrangian multiplier*;

(iii) Ones variables $\dot{\mathbf{q}}_{n+1}$ and λ_{n+1} are calculated, according to Eq. (3) a new kinematic load multiplier (μ_k^{n+1}) follows, as well as coefficient matrix \mathbf{S}_{n+1} governing the global internal power dissipation of the structure.

The whole procedure assumes an iterative configuration in the repetition of steps (ii)-(iii). It stops when: (a) the number of “inactive” modes has to remain constant for 10 iterations; (b) the relative change of the load multiplier from a step to another is lower than 10^{-3} .

In Ferrari et al. [15] a comprehensive description of the computational formulation is provided, along with the proof of convergence of the iterative procedure and some interesting remarks concerning the influence of computing round-off errors on the effectiveness of the algorithm. The latter turns out to be essential in order to deal with 3D large-scale macro-structures, endowed with a large number of dofs and associated potentially active plastic joints, as the one herein presented as a benchmark structure.

3. Large-scale structural numerical simulations

3.1. Benchmark structure

The benchmark structure considered in the present paper is represented by the parabolic arch of the Paderno d’Adda bridge, an iron railway viaduct that crosses the Adda river between Paderno d’Adda (LC) and Calusco d’Adda (BG) at a height of approximately 85 m from water. It allows for connecting the provinces of Lecco and Bergamo, near Milano, in Lombardia, northern Italy (Figure 1). The viaduct, co-aged of most celebrated Tour Eiffel, and rather similar to that in contemporary structural features, was quickly constructed between 1887 and 1889 and is one of the very first great iron constructions designed through the practical application of the so-called “Theory of the Ellipse of Elasticity” (Ferrari and Rizzi [17]), a graphic-analytic method of structural analysis that was developed in the 19th century. The bridge is made of a wrought iron material; the structural elements are interconnected by riveted joints. It is composed of: an elegant and robust doubly-built-in parabolic arch of about 150 m of horizontal span and 37.5 m of vertical rise; vertical bearing piers with a height up to 31.5 m; an upper continuous beam of 266 m of length. The main upper continuous beam, 5 m wide and 6.25 m high, is formed by a metallic truss-frame supported by nine bearings, four of which are supported by the arch. Wide documentations on the historic bridge are available in Ferrari and Rizzi [17], Ferrari et al. [14] and references quoted therein.

For the finalities of the present paper, the homemade FEM model of the arch of the bridge has been extracted from a preassembled FEM model of the bridge, earlier implemented within commercial FEM code ABAQUS[®]. It has been constituted by assembling a 3D truss-frame with beam elements, mutually built-in at the nodes. The 3D truss-frame of the arch consists of two planar parabolic trusses laying into two inclined planes (of an angle $\alpha \approx \pm 8.63^\circ$ to the vertical), symmetrically located with respect to the vertical longitudinal plane of the viaduct. The inclined planes are placed at a relative distance of 5.096 m at the keystone. A single arch profile is considered in each inclined plane, with an arch body that accounts for the true presence of two secondary twin inclined arches, on the two sides of such an inclined plane. The truss nodes are linked to each other through a reticular system that corresponds to the true bracing system of the arch. The arch presents some additional reinforcing plates between the vertical bars in each of the secondary twin inclined arches, placed at the locations of the arch/bearing connections. These plates have not been explicitly represented in the FEM model

of the structure. To comply with this, the cross sections of the limiting vertical bars contouring the stiffening plates have been endowed with larger geometrical characteristics. The FEM model of the arch of the bridge is comprised of 1051 beam elements and 342 nodes and is endowed with the following material properties, characteristic of a wrought iron material (SNOS [18], Nascè et al. [19]): Young's modulus $E=17 \cdot 10^6 \text{ tons/m}^2 \approx 170 \text{ GPa}$; Poisson's ratio $\nu=0.3$ (corresponding shear modulus $G=6.54 \cdot 10^6 \text{ tons/m}^2 \approx 65.4 \text{ GPa}$); mass density $\rho=7.7 \text{ tons/m}^3$. Despite that yield limit characteristics of the material could be set to those that may be typically reported for an iron material (Nascè et al. [19]), the yield limit assumed in the present computations has been conservatively taken coincident with the allowable working stress imposed by the builder at design stage (SNOS [18]), namely $\sigma_y=6.00 \text{ kg/mm}^2 \approx 60 \text{ MPa}$ (and $\tau_y=\sigma_y^{1/3}=3.46 \text{ kg/mm}^2 \approx 34.6 \text{ MPa}$). The FEM model of the arch of the Paderno d'Adda bridge is depicted in Figure 2, which forms the basis for the elastoplastic model with potentially active plastic joints located at the extremes of each beam finite element.



Figure 1: Contemporary view of the Paderno d'Adda bridge (1889) from the right bank.

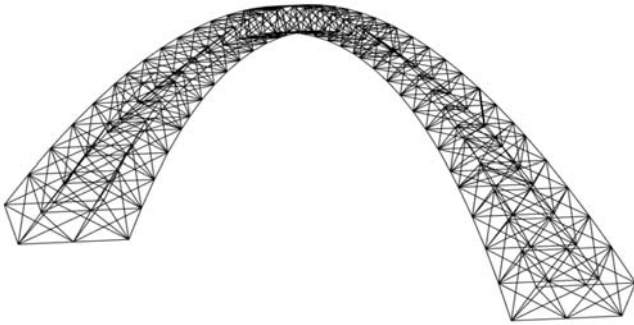


Figure 2: FEM model of the arch of the Paderno d'Adda bridge.

3.2. Loading configuration

The loads considered in the performed numerical simulations have been set with reference to the static try-out railway loading conditions on the Paderno d'Adda bridge (SNOS [18], Nascè et al. [19]). These tests were carried-out using locomotives with tender, each of 83 tons of weight, corresponding to a uniformly distributed load on the beam of about $q=5.1 \text{ tons/m}$. Such distributed live load leads to elastic reactions on the arch, at its interfaces with the piers and the upper beam, equal to $P_1=163.5 \text{ tons}$, $P_2=171.3 \text{ tons}$, $P_3=168.7 \text{ tons}$, $P_4=171.3 \text{ tons}$, for

a total live load of $Q=674.8$ tons just on the arch (Figure 3). These values of P_i come from the elastic solution of a nine-bearing continuous beam, with firm supports, and are here assumed to be representative of the load distribution directly lying on the arch, when a uniform load is acting on the above upper continuous beam (Ferrari et al. [13]).

In the numerical simulations, only above-mentioned live loads P_i and associated total load Q have been considered to be affected by a load multiplier. The self-weight of the structure has instead been treated as a pre-imposed permanent load; namely, this has not been affected by the load multiplier. In particular, the self-weight of the upper continuous beam and the piers on the arch has been considered through loads directly applied to the arch at the arch/beam and arch/piers interfaces. To determine such permanent loads, the upper truss structure has been considered as a continuous beam supported by nine bearings, subjected to a uniformly-distributed load representing the weight of the upper beam and set equal to 6.61 tons/m (SNOS [18]). Therefore, vertical reaction forces at the bearings located at the level of the arch/piers and arch/beam interfaces have been calculated. The two reactions at the level of the arch/beam interfaces (P_2 and P_3 in Figure 3) have then been directly applied to the arch of the bridge, meanwhile the two reactions at the level of the arch/piers interfaces (P_1 and P_4 in Figure 3) have been incremented by the weight of the piers resting on the arch, given equal to 22 tons (SNOS [18]). Permanent resultants P_1 - P_4 applied to the arch, due only to the self-weight of the upper continuous beam and the piers on the arch (not affected by the load multiplier), therefore result equal to $P_1=233.9$ tons, $P_2=222.0$ tons, $P_3=218.7$ tons, $P_4=244.0$ tons.

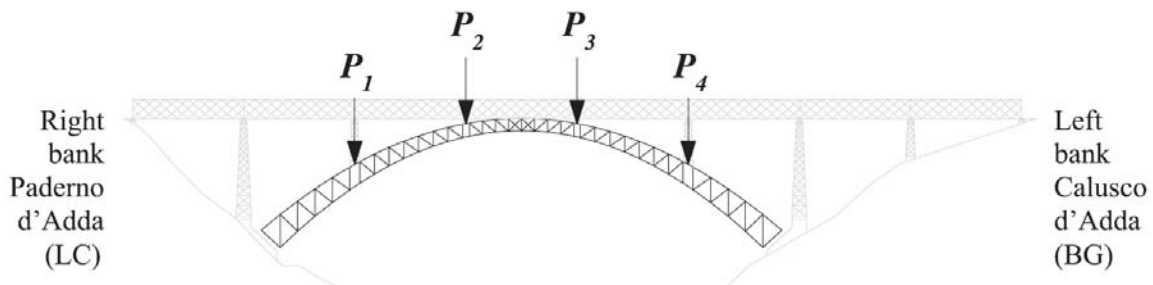


Figure 3: Scheme of the considered static load configuration (view from down-stream), with loads P_i applied on the arch structure at the arch/piers and arch/beam interfaces.

3.3. Numerical results

The results in terms of elastoplastic load-carrying capacity of the bridge's arch obtained with the above-discussed (Section 2) numerical algorithms of Limit Analysis are consistently shown in Table 1. Moreover, the mechanical elastoplastic response of the arch substructure is depicted in Figures 4-6.

Table 1: Collapse load multipliers for the benchmark structure.

Method	Collapse load multiplier	Limit state
Evolutionary	4.17	First null eigenvalue of stiffness matrix
Kinematic	4.22	Formation of a collapse mechanism

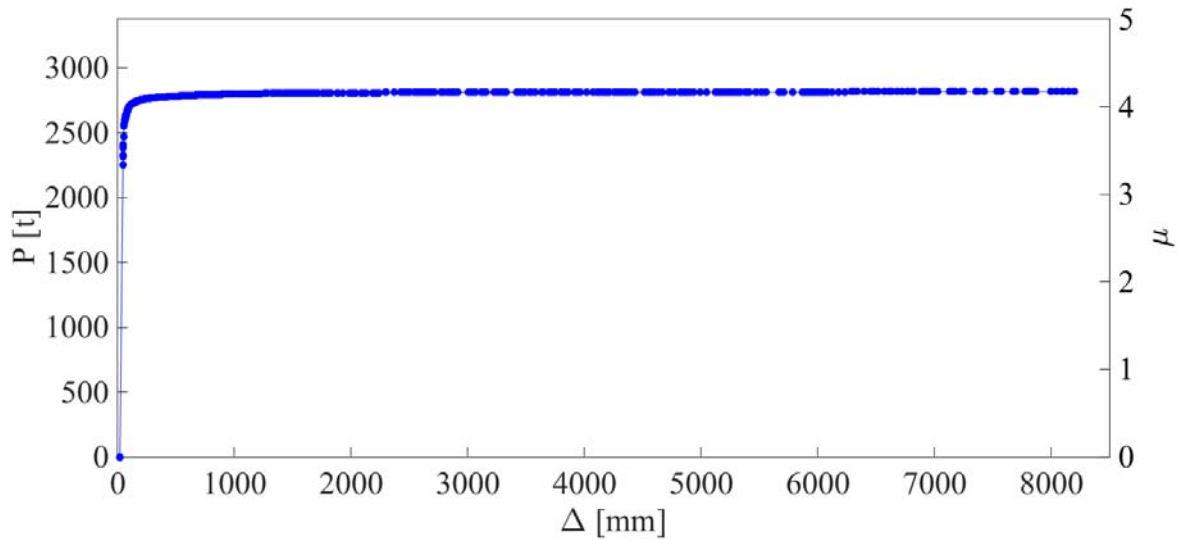


Figure 4: Representation of the characteristic piece-wise linear load–displacement response curve.

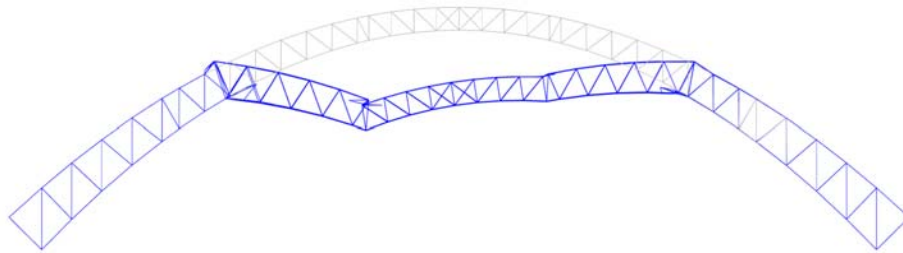


Figure 5: Collapse mechanism of the arch of the Paderno d'Adda bridge by the kinematic algorithm.

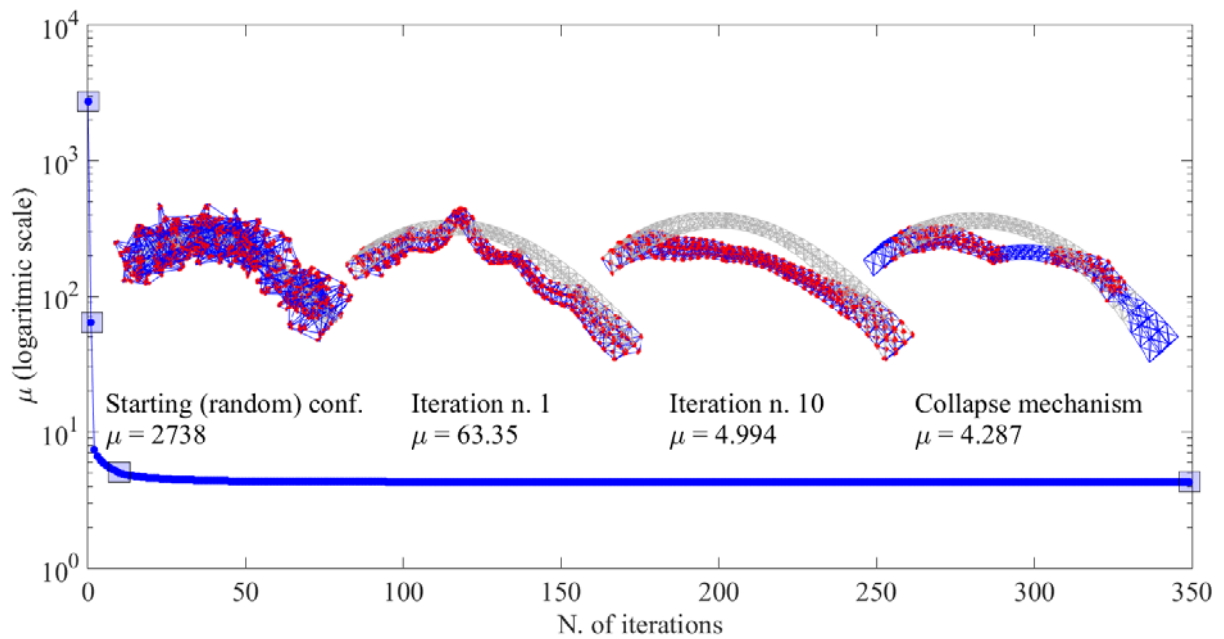


Figure 6: Collapse load multiplier and plastic mechanism estimation along the kinematic iterative procedure.

The numerical evaluation of the collapse load multiplier reported in Table 1 shows a minor discrepancy between the upper-bound value obtained by the kinematic method and the estimated value achieved by the evolutive analysis (a static evaluation, in essence, and as set at the very earliest singularity of the tangent stiffness matrix). This difference (likely forming a fork delimiting the real numerical collapse load multiplier) may be due to round-off errors and adopted numerical tolerances within the kinematic approach, possibly being linked to the diffused amount of very small plastic deformations in several deactivated joints, along the iterations. This may require further inspections and refinements of the kinematic algorithm, in order to handle such large-scale 3D truss-frame structures.

Figure 4 reports the characteristic piece-wise linear load/displacement response curve of the arch obtained from the evolutive algorithm (Section 2.1), showing a considerable global structural ductility. In particular, the horizontal axis depicts the vertical displacement (Δ) of the node that, in the end, has shown the maximum displacement at incipient collapse; the left vertical axis reports total amplified live load $P=\mu Q$, where μ is the load multiplier related to the incremental solution of the non-linear elastoplastic analysis; the right vertical axis also depicts load multiplier μ . Therefore, in the plot, the response curve for the loading configuration can be read on the left or on the right axis, equivalently. The end point of the $P-\Delta$ curve refers to the so-estimated “exact” collapse of the structure in terms of first vanishing minimum eigenvalue of the tangent stiffness matrix of the structure (Section 2.1). Notice that in this plot the non-zero initial displacement (at $P=0$) is due to self-weight only, namely to a pre-imposed permanent load not affected by the load multiplier. In this case, the computing time to achieve the collapse solution was about 1100 s. The algorithm has been implemented and run as a non-compiled code within MATLAB[®], under a Windows 10 operating system, on a Dell laptop endowed with an Intel Core i7-6500U Processor, clock at 2.50 GHz and 16 GB RAM.

Figure 5 also depicts the deformed configuration of the structure at incipient collapse (namely, the plastic collapse mechanism), as obtained by the kinematic LA algorithm (Section 2.2), which is rather consistent with that derived from the evolutive program (Section 2.1).

Figure 6 further illustrates the results related to the kinematic algorithm (Section 2.2). It displays the collapse load multiplier computed during the iterative procedure, and the associated estimated collapse mechanism along the iterations. In the picture, it is possible to appreciate how the implemented algorithm is capable to quickly and easily achieve convergence. In fact, the collapse mechanism is almost already achieved at the tenth iteration, and in already about 40 iterations the kinematic load multiplier precipitates on the collapse one; after that, the load multiplier turns out to be almost flat, at an increasing number of iterations. In this case, the computing time to achieve the collapse solution by the direct kinematic method (in about 350 iterations) was nearly 37 s, on the same computer platform as described above, thus with a saving of more than 96% of the computational time employed for the corresponding complete evolutive elastoplastic approach (1100 s).

Conclusions

The present paper has attempted a comprehensive computational elastoplastic structural analysis, truly loyal to the principles of Limit Analysis, in the context of large-scale 3D truss-frame structures, with reference to the elastoplastic response of a strategic historic infrastructure within the local territory (Paderno d’Adda bridge, 1889), in order to investigate its potential performance in terms of LA limit states, with focus on the supporting parabolic arch.

Two approaches have been employed, compared and cross-connected, in view of deciphering the resources of the fundamental arch-bearing mechanism of the iron bridge, toward the limit state of plastic collapse, as follows: a reconstruction of the complete evolutive response up to collapse, with the sequence of activation of the plastic joints in the various members of the boxed-form arch structure and the associated tracing of the global load-displacement curve; a direct determination of the collapse characteristics, in terms of collapse load multiplier and plastic mechanism.

Both LA methods of analysis consistently run and effectively perform, despite for the rather considerable number of dofs considered within the computation (more than 4,000). A true match is displayed for the predictions of plastic collapse, with the kinematic iterative algorithm showing an impressive performance in really precipitating from above onto the collapse load multiplier, and with a plastic mechanism that rapidly adjusts, in very few iterations, to the collapse mode.

As for the interpretation of the achieved results on such a crucial and beautiful historic infrastructure, the arch is revealed by both methods to constitute a well-set fundamental structural element, with considerable resources in terms of plastic collapse, testifying the mastering of the methods of structural design and execution by the art of metallic carpentry at the time, despite for being directly conceived on the basis of (graphic-analytic) elastic methods of analysis only (see Ferrari and Rizzi [17]). This brings really good news, at present stage, in terms of debating possible future destinations of the monumental infrastructure.

These new LA computational methodologies may open up the way for LA to regaining a new, considerable momentum in the structural analysis of large-scale structures, of both a new design concept and historic, to be preserved, ones, and with new challenging targets in terms of structural optimization, as for structural design or form-finding quests, given the prompt availability of the mechanical calculation, within a possible optimization loop that may consider variable structural characteristics and trace (optimize) the corresponding variation of the elastoplastic response and the attached collapse features.

References

- [1] Drucker DC, Prager W, Greenberg HJ (1952) Extended limit design theorems for continuous media. *Quarterly of Applied Mathematics*, 9(4):381–389.
- [2] Massonet CH, Save M (1978) In: Nelissen, B. (Ed.), *Calcul Plastique des Constructions*. Angleur, Liège, Belgium.
- [3] Kaliszky S (1989) *Plasticity: Theory and Engineering Applications*, Elsevier, Amsterdam, Netherlands.
- [4] Lubliner J (1990) *Plasticity Theory*, McMillan Publisher, New York.
- [5] Jirasek M, Bazant ZP (2002) *Inelastic Analysis of Structures*, Wiley, Chichester, U.K.
- [6] Maier G, Carvelli V, Cocchetti G (2000) On direct methods for shakedown and limit analysis. *European Journal of Mechanics - A/Solids*, 19(Special Issue - 4th EUROMECH Solid Mechanics Conference, Plenary Lectures, Metz, France, June 26-30, 2000), S79–S100.
- [7] Cocchetti G, Maier G (2003) Elastic-plastic and limit-state analyses of frames with softening plastic-hinge models by mathematical programming. *International Journal of Solids and Structures*, 40(25):7219–7244.
- [8] Tangaramvong, S., Tin-Loi, F. (2007) A complementarity approach for elastoplastic analysis of strain softening frames under combined bending and axial force. *Engineering Structures*, 29(5), 742–753.
- [9] Lògò J, Kaliszky S, Hjjaj M, Movahredi Rad M (2008) Plastic Limit and Shakedown Analysis of Elastoplastic Steel Frames with Semirigid Connections. In Proc. of *Design, Fabrication and Economy of Welded Structures*, Eds. Károly Jármai and József Farkas, Miskolc, Hungary, April 24-26, 2008, pp. 237–244.
- [10] Skordeli M-AA, Bisbos CD (2010) Limit and shakedown analysis of 3D steel frames via approximate ellipsoidal yield surfaces. *Engineering Structures*, 32(6):1556–1567.

- [11] Bleyer J, Buhan P (2013) Yield surface approximation for lower and upper bound yield design of 3D composite frame structures. *Computers and Structures*, 129(December 2013):86–98.
- [12] Nikolaou KD, Georgiadis K, Bisbos CD (2016) Lower bound limit analysis of 2D steel frames with foundation-structure interaction. *Engineering Structures*, 118(1 July 2016):41–54.
- [13] Ferrari R, Cocchetti G, Rizzi E (2016) Limit Analysis of a historical iron arch bridge. Formulation and computational implementation. *Computers and Structures*, 175(2016):184–196, doi: 10.1016/j.compstruc.2016.05.007.
- [14] Ferrari R, Cocchetti G, Rizzi E (2017) Computational elastoplastic Limit Analysis of the Paderno d'Adda bridge (Italy, 1889). *Archives of Civil and Mechanical Engineering*, 18(1):291–310, doi:10.1016/j.acme.2017.05.002.
- [15] Ferrari R, Cocchetti G, Rizzi E (2018) Effective iterative algorithm for the Limit Analysis of truss-frame structures by a kinematic approach. *Computers and Structures*, 197(15 February 2018):28–41, doi:10.1016/j.compstruc.2017.11.018.
- [16] Zhang P, Lu M, Hwang K (1991) A mathematical programming algorithm for limit analysis. *Acta Mechanica Sinica* 7(3):267–74.
- [17] Ferrari R., Rizzi E. (2008) On the theory of the ellipse of elasticity as a natural discretisation method in the design of Paderno d'Adda Bridge (Italy). Chapter 66 in *Structural Analysis of Historic Construction – Preserving Safety and Significance*, In Proc. of *6th International Conference on Structural Analysis of Historic Construction (SAHC08)*, D. D'Ayala and E. Fodde (Eds.), Bath, UK, July 2–4, 2008, CRC Press, Taylor & Francis Group, London, print ISBN: 978-0-415-46872-5, pp. 583–591; eBook ISBN: 978-1-4398-2822-9, doi:10.1201-9781439828229.ch66.
- [18] Società Nazionale delle Officine di Savigliano (1889). *Viadotto di Paderno sull'Adda (Ferrovia Ponte S. Pietro-Seregno)*. Torino: Tip. e Lit. Camilla e Bertolero.
- [19] Nascè V, Zorgno AM, Bertolini C, Carbone VI, Pistone G, Roccati R (1984). Il ponte di Paderno: storia e struttura - Conservazione dell'architettura in ferro. *Restauro*, Anno XIII, n. 73-74, 215 pages.